*The Annals of the University Dunarea de Jos of Galati*
*Fascicle VI – Food Technology (2022), 46(2), 35-49*

**ORIGINAL RESEARCH PAPER**

# THE STABILITY OF WHEY PROTEIN-STABILIZED RED PALM OIL EMULSION FROM A RHEOLOGICAL PERSPECTIVE

VALLERINA ARMETHA[1,2], PURWIYATNO HARIYADI*[,1,2], AZIS BOING SITANGGANG[1], SRI YULIANI[3]

[1] *Department of Food Science and Technology, Faculty of Agricultural Engineering and Technology, IPB University, Bogor 16680, Indonesia*

[2] *Southeast Asian Food and Agricultural Science and Technology (SEAFAST) Center, IPB University, Bogor 16680, Indonesia*

[3] *Indonesian Centre for Agricultural Postharvest Research and Development, Indonesian Agency for Agricultural Research and Development, Bogor 16122, Indonesia*

*Corresponding author: phariyadi@apps.ipb.ac.id

Received on 31 May 2022
Revised on 21 July 2022

**Abstract**

The objective of this study was to investigate into the physical stability of whey protein (WP)-stabilized red palm oil (RPO) emulsions based on rheological properties such flow behaviour, viscoelastic properties, apparent viscosity ($\eta_{app}$), and linear viscoelastic range limits (*LVE*). RPO emulsification was stabilized by three types WP with different protein content, notably WPI90, WPC80, and WPC76, and the influence of WP type and concentration (2.5-15%) was evaluated. Utilizing the type and concentration of WP used, RPO emulsions with good apparent thermodynamic stability could be formed. All of the emulsions showed shear-thinning flow behaviour with viscous properties ($G'' >> G'$). However, as a result of the different WP types and concentrations utilized, the emulsions produced had varied kinetic stability and rheological properties. Droplet characteristics, such as $D_{10}$, $D_{50}$, and $D_{90}$, $\zeta$ potential, and electrical conductivity were determined, and rheological data gained corresponded with these properties to explain emulsion stability. The *LVE* value reflected the stability of the produced emulsions as well as the $\eta_{app}$ difference. The emulsion stabilized with 15% of WPC76 had optimum physical stability in this study, with an *LVE* of 7.9%. This study demonstrate that rheological characterization can be employed to assess the stability of WP-stabilized RPO emulsions.

**Keywords**: Casson fluid, emulsion stability, Herschel-Bulkley fluid, red palm oil (RPO), rheology

https://doi.org/10.35219/foodtechnology.2022.2.03

## Introduction

An oil-in-water (O/W) emulsion is a promising carrier system for enhancing the oxidative stability of lipophilic-bioactive compounds (Boon, 2009; McClements *et al*., 2007). However, good emulsion physical stability is necessary to obtain a sufficiently strong barrier for encapsulating the intended bioactive (Boon, 2009; McClements *et al*., 2007). Dairy protein-stabilized O/W emulsions have recently been widely researched as carrier systems. Dairy protein-based emulsifiers (*e.g.* milk protein, whey protein (WP), caseins, and their corresponding fractions) may also have additional benefits for emulsions system, such as electrostatic repulsive force and steric stabilization, bioactive binding to improve bioactive stability, fulfilling the demand for healthy natural materials, and adding nutritional value (Ha *et al*., 2019; McClements, 2004).

Red palm oil (RPO) is a nutrient-dense edible oil rich in lipophilic-bioactive compounds, such as carotenoids (*i.e.* β- and α-carotene), vitamin E (tocotrienols and tocopherols), phytosterols, and ubiquinones (Loganathan *et al*., 2017). Because of its remarkable antioxidant and provitamin A activities, RPO possesses great promise to be used as a source of natural lipophilic-bioactive compounds. The lipophilic-bioactives present in the RPO matrix are also considerably more bioaccessible and bioavailable than extracted lipophilic-bioactives. However, the utilization of RPO bioactives is still limited due to their poor storage stability. RPO is susceptible to oxidation as a result of exposure to environmental factors such as oxygen, light, and other oxidizing substances (Boon, 2009; Burri, 2012). As a consequence, efforts need to be made to enhance RPO stability as well as its bioactives, one of which is to eliminate the sensitizers.

WP-based emulsifiers have been reported to produce stable O/W palm emulsions, and the emulsions could enhance the stability of bioactive components, such as β-carotene and α-tocopherol (Mohamad *et al*., 2017; Ricaurte *et al*., 2016). The protein content and nature of the WP contributes to its excellent emulsification capacity. However, studies on WP-based emulsifiers for O/W RPO emulsion stabilization is still limited. Our recent work shown that WP-based emulsifiers could form a stable RPO emulsion, however the prior study was still constrained to visual observations (e.g., appearance stability, creaming index) (Armetha *et al*., 2022). Of course, an emulsion with good thermodynamic and kinetic stability is necessary to maximize the stability of lipophilic-bioactives. The evaluation of the physical stability of the WP-stabilized emulsion itself becomes important before assessing the oxidative stability of the emulsified bioactives.

Rheological characterizations can provide information regarding the physical stability of an emulsion (Drapala *et al*., 2018; Tadros, 2013; Yang *et al*., 2020). Rheological data might be used to evaluate the system design of a biopolymer-stabilized emulsion as well as its stability throughout the presence of external forces (Drapala *et al*., 2017; Sun and Gunasekaran, 2009; Yang *et al*., 2020). Rheology, according to Drapala *et al*. (2018), could give an indirect depiction of the shape or form and size of emulsion constituents such as oil globules, protein aggregates, interface systems, and their interactions. Therefore, emulsion rheology is considered to be capable of evaluating the strength of the emulsion's physical barrier formed, which explains its stability. Based on the preceding, the main objective of this work was to investigate the physical stability of WP-stabilized RPO emulsions as influenced by WP type and concentration based on their rheological properties.

## Materials and methods

### *Materials*

Three types of commercially available WP with different protein content (WP Isolate (WPI) Provon® 190, WP Concentrate (WPC) Avonlac™ 180, and WPC OptiSol® 1007 denoted as WPI90, WPC80, and WPC76, respectively) were obtained from Glanbia Nutritionals Singapore Pte. Ltd. (Singapore). RPO (carotenoid content >500 ppm, iodine number 55–58, free fatty acids <1%, and peroxide number <1 mEq $O_2$/kg) was obtained from the Indonesian Oil Palm Research Institute (Medan, Indonesia). Deionized water was purchased from Hach Lange GmbH (Germany). Other chemicals used in this study were of proanalytical grade and purchased from Merck KGaA (Darmstadt, Germany).

### *Emulsification of WP-based RPO emulsions*

Emulsification was performed using a previous reported method (Armetha *et al*., 2022). The continuous phase was initially prepared. Each WP product (WPI90, WPC80, or WPC76) was dissolved in deionized water to achieve the desired concentrations (2.5%, 5%, 10%, and 15% w/v) of WP solution containing 0.02% (w/v) sodium azide. The mixture was constantly stirred at 750 rpm (IKA C-MAG HS7, Staufen, Germany) for 1 h at room temperature before being stored at 4°C ± 1°C overnight (±18–20 h). Afterward, the continuous phase was gradually added to RPO to form 30% (v/v) RPO emulsions employing a phase inversion technique during the first homogenization step. In the first homogenization step, a rotor-stator homogenizer (Silverson L4r; Silverson Machines, Ltd, Bucks, UK) was set at 9000 rpm for 2 min. After that, the speed increased to 18000 rpm for 5 min. After emulsification, WP concentration in the system was estimated to be 1.75%, 3.50%, 7.00%, and 10.50% (w/v). The RPO emulsions were produced in duplicate.

### *Rheological characterization*

A modular compact rheometer (MCR) 92 series (Anton Paar GmbH, Austria) was used for rheological characterization in this work. Measurements were performed using a cone-plate probe (CP) 50-1° with a 0.1 mm gap at 25°C following to the referenced method with modification. The flow curve obtained from the rotational shear method was analysed by mapping the shear stress ($\tau$) as a function of the shear rate ($\dot{\gamma}$), and the viscosity ($\eta$) curve was examined by mapping the apparent viscosity ($\eta_{app}$) as a function of the $\dot{\gamma}$; both at $\dot{\gamma}$ ramp from $10^{-1}$ to $10^3$ $s^{-1}$ at 25 analysis points. Furthermore, $\eta_{app}$ among samples was compared after being tested at a $\dot{\gamma}$ of $10^2$ $s^{-1}$ (Mantovani *et al*., 2013). The flow curve was then assessed to forecast the flow behaviour model of the emulsions using the equations of Bingham (Equation 1), Casson (Equation 2), Power-law (Equation 3), and Herschel–Bulkley (Equation 4) (Barnes, 2000).

$$\tau = \tau_0 + \eta \cdot \dot{\gamma} \quad (1)$$

$$\tau^{\frac{1}{2}} = \tau_0^{\frac{1}{2}} + (\eta \cdot \dot{\gamma})^{\frac{1}{2}} \quad (2)$$

$$\tau = K \cdot \dot{\gamma}^n \quad (3)$$

$$\tau = \tau_0 + K \cdot \dot{\gamma}^n \quad (4)$$

where $\tau$ is the shear stress, $\tau_0$ is the yield stress, $\dot{\gamma}$ is the shear rate, $\eta$ is the Bingham plastic viscosity (equation 1), $\eta$ the Casson rheological constant (Equation 2), K and n are the flow consistency index and the flow behaviour index for Power-law fluid model (Equation 3), and K and n are the flow consistency index and the flow behaviour index for Herschel-Bulkley (HB) fluid model (Equation 4), respectively.

Next, the dynamic amplitude oscillatory shear method was used to examine the viscoelasticity of the emulsions. The amplitude sweep test rheogram was analysed by mapping the loss (viscous) modulus ($G''$) and storage (elastic) modulus ($G'$) functions of shear strain from 0.1% to 1000% at frequency of 1 $s^{-1}$ at 41 analysis points (Hinderink *et al.*, 2021). Each measurement was carried out twice using a logarithmic ramp mode.

***Droplet characterization***

The RPO emulsion droplets were characterized with respect to average hydrodynamic diameter (average droplet size–ADS), droplet size distribution (*i.e.* $D_{10}$, $D_{50}$, and $D_{90}$), ζ potential, and electrical conductivity ($k$). $D_{10}$, $D_{50}$, and $D_{90}$ represent droplet sizes corresponding to 10%, 50%, and 90% cumulative undersize distributions, respectively. A Litesizer™ 500 (Anton Paar GmbH, Austria) BM 10 module was used at a shooting angle of 175° (Anton Paar, 2017). The measurements were carried out in triplicates.

***Statistical analysis***

The results were reported as means ± standard deviations unless otherwise noted. The collected data were analysed using an ANOVA with Duncan's multiple range post-hoc test, and the correlations between chosen parameters were analysed through Pearson correlation; both analyses were performed with SPSS 26.0 software (SPSS Inc., Chicago, IL, USA) was used for both analyses. A P-value of < 0.05 was considered significant.

## Results and discussion

***Droplet characteristics and apparent viscosity of emulsions***

The droplet characteristics (*i.e.* $D_{10}$, $D_{50}$, and $D_{90}$, ζ potential, and $k$) and $\eta_{app}$ of the RPO emulsions produced in this study were influenced by the type and concentration of WP used (Table 1, Figure 1). The ADS values of the emulsions significantly decreased as the WP concentration increased (Figure 1). This trend was also significantly noticeable in the particle size distribution ($D_{10}$, $D_{50}$, and $D_{90}$) (Table 1).

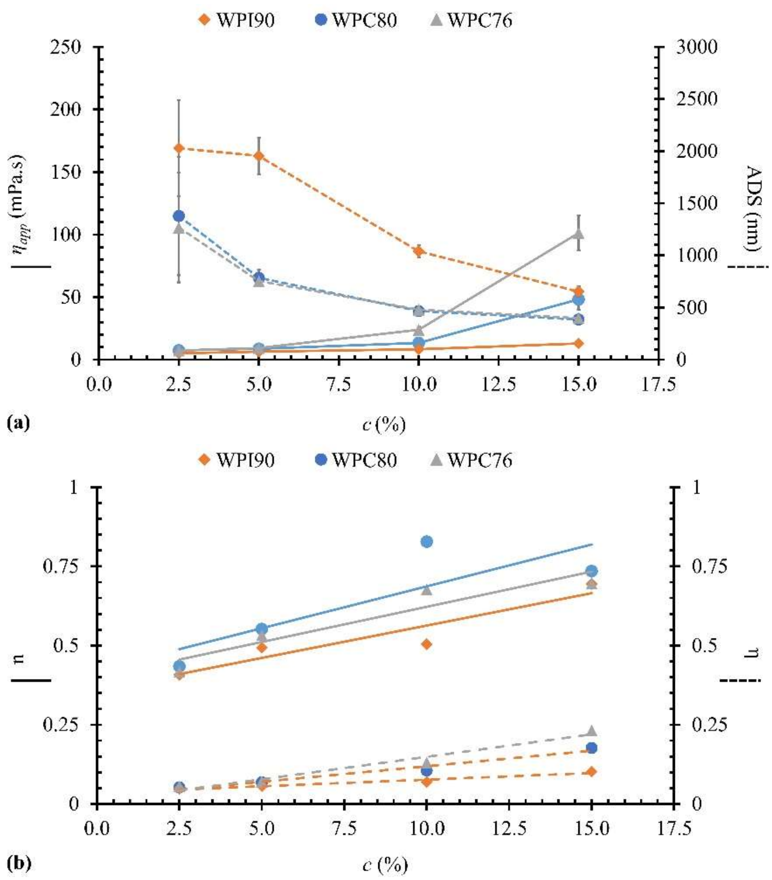


**Figure 1.** Apparent viscosity ($\eta_{app}$) and average droplet size (ADS) (a) and the Casson rheological constant (η) and flow behaviour index (n) calculated using Equation 2 (b) of the RPO emulsions as a function of WP concentration ($c$).

The ζ potential is a value that measures the density of the droplet surface charge. The ζ potential can be used to quantify the power of repulsive interaction between droplet surfaces (steric hindrance) (Ha *et al.*, 2019; McClements, 2007). In this study, the ζ potential of the emulsions was negatively charged and was not significantly influenced by the WP type and concentration. However, the observed trend in the data supports the hypothesis that the concentration of WP influences the ζ potential of the emulsions. Based on the data, the ζ potential were less negative as WPC80 and WPC76 concentrations increased, but this tendency was not observed when WPI90 was used. The negatively charged characteristic is caused by protein's negative charge at physiological pH values above its isoelectric point. The isoelectric point of WP was 4.5 (Pelegrine and Gasparetto, 2005), whereas the pH of deionized water used as the continuous phase was almost seven. However, the ζ potential of emulsions became less negative as WPC76 concentration increased. The observed phenomenon is thought to be caused by the nature of protein of the WP used (i.e., protein ionization state on the system). In contrast, Zhou *et al.* (2020) and Sun and Gunasekaran (2009) reported that the ζ potential become more negative when WP concentration increased. Meanwhile, other research found no significant influence of protein concentration on ζ potential at the same temperature, pH, and emulsification conditions (Adjonu *et al*., 2014; Hinderink *et al*., 2021). Yang *et al.* (2020) reported that ζ potential might be altered by emulsifier type, which can be explained by the nature of the protein used (*i.e.* the amount of hydrophobic region and molecular structure (folded or unfolded)); which is consistent with this work findings.

**Table 1.** Droplet size distribution ($D_{10}$, $D_{50}$, and $D_{90}$), ζ potential, and electrical conductivity (*k*) of the RPO emulsions at different WP concentrations (*c*).

| WP type | *c* (%) | $D_{10}$ (nm) | $D_{50}$ (nm) | $D_{90}$ (nm) | ζ (mV) | *k* (mS/cm) |
|---|---|---|---|---|---|---|
| WPI90 | 2.5 | $1266.80 \pm 383.91^{a,d}$ | $1710.37 \pm 413.28^{a,d}$ | $2347.78 \pm 466.03^{a,d}$ | $-18.34 \pm 7.27^{a,d}$ | $0.57 \pm 0.01^{a,d}$ |
| | 5 | $1177.33 \pm 53.44^{a,d,e}$ | $1621.84 \pm 74.86^{a,d,e}$ | $2307.37 \pm 312.60^{a,d,e}$ | $-20.75 \pm 11.27^{a,d}$ | $0.58 \pm 0.01^{a,d}$ |
| | 10 | $599.02 \pm 57.18^{a,e}$ | $1080.65 \pm 265.86^{a,e,f}$ | $2003.15 \pm 1065.00^{a,e}$ | $-15.90 \pm 6.03^{a,d}$ | $0.61 \pm 0.01^{a,e}$ |
| | 15 | $327.98 \pm 94.72^{a,e}$ | $660.99 \pm 105.85^{a,f}$ | $1054.67 \pm 242.04^{a,e}$ | $-11.39 \pm 10.09^{a,d}$ | $0.64 \pm 0.01^{a,e}$ |
| WPC80 | 2.5 | $932.14 \pm 429.15^{a,b,d}$ | $1468.95 \pm 667.20^{a,d}$ | $2133.66 \pm 960.76^{a,d}$ | $-21.61 \pm 1.11^{a,d}$ | $0.59 \pm 0.01^{a,d}$ |
| | 5 | $344.77 \pm 107.26^{a,b,d,e}$ | $822.32 \pm 86.05^{a,d,e}$ | $1501.14 \pm 158.51^{a,d,e}$ | $-14.63 \pm 9.82^{a,d}$ | $0.59 \pm 0.01^{a,d}$ |
| | 10 | $260.66 \pm 25.34^{a,b,e}$ | $488.90 \pm 14.74^{a,e,f}$ | $791.45 \pm 37.03^{a,e}$ | $-27.30 \pm 11.33^{a,d}$ | $0.61 \pm 0.01^{a,e}$ |
| | 15 | $219.88 \pm 22.70^{a,b,e}$ | $369.38 \pm 15.26^{a,f}$ | $601.20 \pm 64.68^{a,e}$ | $-5.25 \pm 19.36^{a,d}$ | $0.63 \pm 0.01^{a,e}$ |
| WPC76 | 2.5 | $595.20 \pm 328.59^{b,d}$ | $1404.44 \pm 666.55^{a,d}$ | $2792.76 \pm 1189.85^{a,d}$ | $-21.98 \pm 6.13^{a,d}$ | $0.59 \pm 0.02^{a,d}$ |
| | 5 | $261.23 \pm 101.94^{b,d,e}$ | $855.88 \pm 69.08^{a,d,e}$ | $1476.07 \pm 131.15^{a,d,e}$ | $-17.47 \pm 6.89^{a,d}$ | $0.59 \pm 0.02^{a,d}$ |
| | 10 | $254.81 \pm 27.72^{b,e}$ | $494.67 \pm 38.25^{a,e,f}$ | $828.99 \pm 63.64^{a,e}$ | $-11.72 \pm 5.62^{a,d}$ | $0.64 \pm 0.02^{a,e}$ |
| | 15 | $216.92 \pm 7.76^{b,e}$ | $440.20 \pm 68.42^{a,f}$ | $823.45 \pm 229.38^{a,e}$ | $-6.27 \pm 18.47^{a,d}$ | $0.67 \pm 0.01^{a,e}$ |

*Different superscript letters (a, b, and c) indicate significant difference by factor emulsifier type ($p < 0.05$)

**Different superscript letters (d, e, and f) indicate significant difference by factor emulsifier concentrations ($p<0.05$)

In this work, increasing the WP concentration increased the $\eta_{app}$ and electrical conductivity (*k*) values significantly. Furthermore, the increase in $\eta_{app}$ as a function of WP concentration was higher for the WPC80- and WPC76-stabilized emulsions than for the WPI90-stabilized emulsions, with the WPC76-stabilized emulsion having the highest $\eta_{app}$ increment (Figure 1). In addition, electrical conductivity (*k*) was significantly influenced by the WP concentration rather than WP type. However, the protein content of the WP utilized cannot explain the rise in $\eta_{app}$ because WPC76 (which has the highest $\eta_{app}$) had the lowest protein content (the protein contents based on the specification for WPI90, WPC80, and WPC76 are >90%, >80%, and >76%, respectively). The findings are presumed to be the consequence of an increase in the droplet number or droplet density formed. Based on literature, the droplet size formed might decreases as the emulsifier concentration increases for the same continuous phase volume fraction, resulting in a larger number of droplets formed (McClements, 2004). Pearson's correlation coefficients for $\eta_{app}$ and ADS of WPI90-, WPC80-, and WPC76-stabilized emulsions (0.93, 0.63, and 0.66, respectively) were high (>50%), suggesting a relationship between the two parameters.

In theory, the interaction on the surface of interdroplets becomes stronger when more emulsifying protein is sufficient on the surface (McClements, 2004). Furthermore, a stronger interaction between protein molecules at the surfaces of interdroplets may be producing an increase in number of droplets or droplet density (Figure 2).

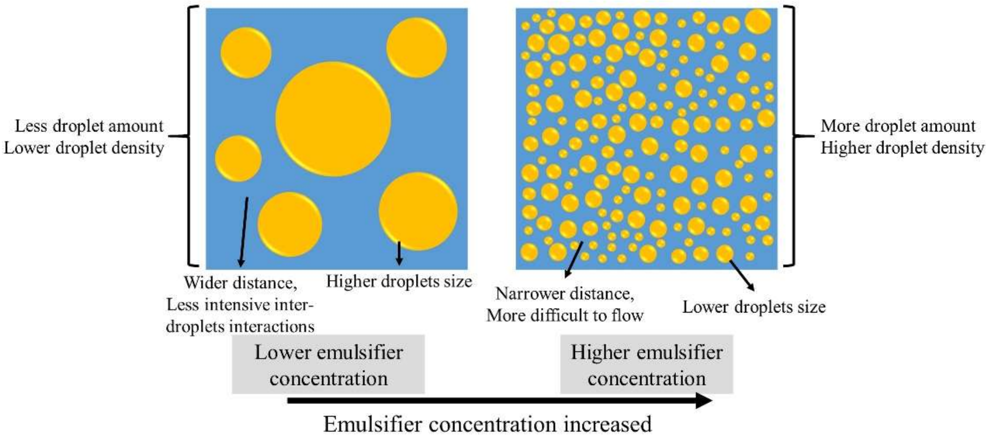


**Figure 2.** Illustration for the relation of emulsifier concentration on the increasing of droplets amount or droplets density formed.

Then, as interaction potential increased and the interactions between interface proteins became stronger, the viscosity and typical rheological parameters increased (Drapala *et al*., 2018; Sun and Gunasekaran, 2009; Tadros, 2013; Xi *et al*., 2019). This congruent with the concepts presented previously by Zhu *et al*. (2020) regarding the shift in rheological emulsion behaviour as the disperse-phase volume fraction increases. A smaller particle size at a high WP concentration may enhance interaction between droplets at denser interdroplets distances. Further, these interaction increase viscosity (Sun and Gunasekaran, 2009; Tadros, 2013; Zhu *et al*., 2020). Zhou *et al*. (2020) also reported that milk fat emulsions stabilized by WPI and WP aggregates exhibited a difference in viscosity increase as influenced by the WP types, which supports the findings of this work. Moreover, McClements (2007) demonstrated that the electrical conductivity ($k$) may be used to describe the density of droplet particles in an emulsion. In this study, the electrical conductivity ($k$) of the RPO emulsions increased as the ADS decreased (Figure 3). This result is then congruent with the theory demonstrated by McClements (2007) and the concept illustrated in Figure 2. The increase in droplets interaction as droplet concentration increases may explain the phenomena of increased the electrical conductivity ($k$) as ADS decreases in this study. According to McClements (2007), electrical conductivity ($k$) can likewise be calculated to droplet concentration using a decent theoretical model or empirical calibration curve.

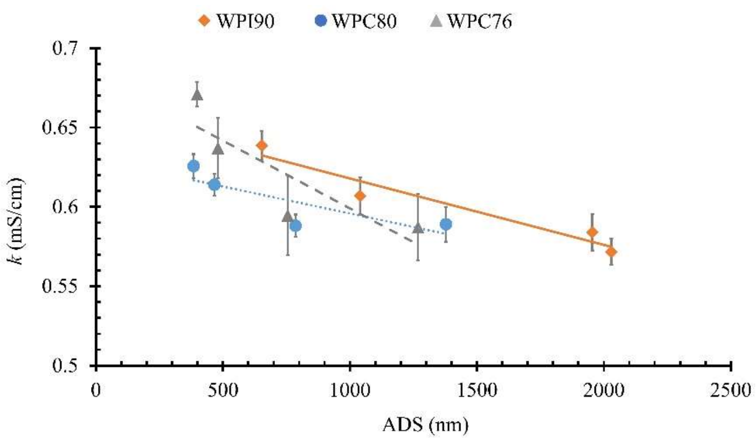


**Figure 3.** Electrical conductivity ($k$) of the RPO emulsions as function of average droplet size (ADS).

The droplet movement caused by Brownian motion and particle interaction may have an effect on the rheology of the system. The movement enhanced flow resistance to external deformation force, as represented by an increase in $\eta_{app}$ (Tadros, 2013). Under isothermal circumstances, emulsion droplet movement can occur for two reasons, which have previously been represented by the Peclet (Pe) number: (i) fluctuations in Brownian molecular motion and (ii) the action of dynamic forces in the flow (Derkach, 2009). A higher particle density is thought to enhance the possibility of droplet–droplet interaction induced by Brownian motion and centrifugal force (i.e., flocculation generation on high particle density emulsions) (Drapala *et al*., 2018; Tadros, 2013), although further study is needed to validate this. Further, previously reported natural characteristics of the emulsion constituents, such as emulsifier solubility and surface activity, might affect the $\eta$ of the emulsion (Castel *et al*., 2017; Domian *et al*., 2015; Tadros, 2013). The continuous phase (WP solution) viscosity is also considered important in determining $\eta_{app}$ (Tadros, 2013).

***Flow behaviour of emulsions***

The RPO emulsions in this study exhibited predominantly shear-thinning behaviour with a yield stress, *i.e.* the non-Newtonian fluid's behaviour with $\tau$ response proportional to the shear strain applied and $\eta$ decreases under shear strain applied (Figures 4 and 5).

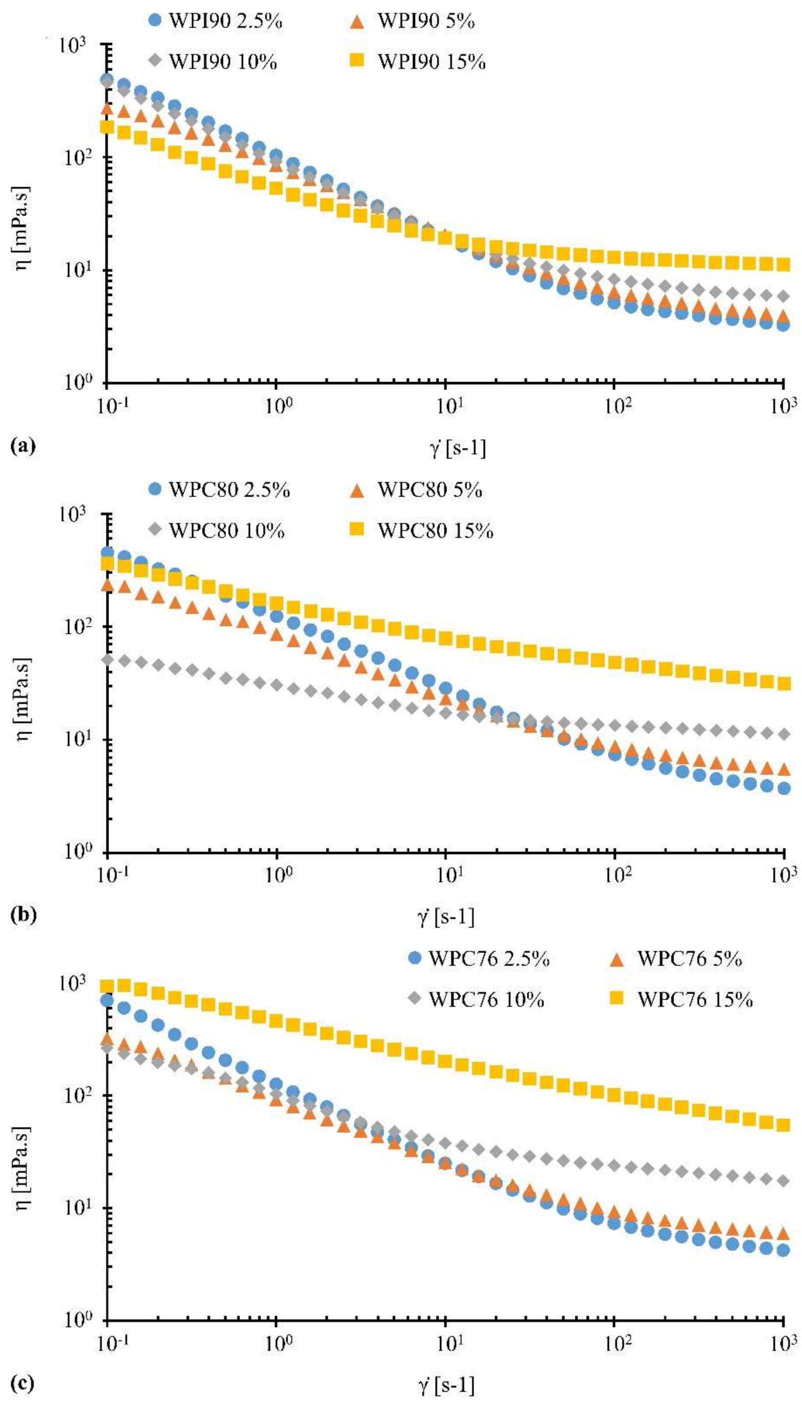


**Figure 4.** Viscosity curves of the RPO emulsions when stabilized by WPI90 (a), WPC80 (b), and WPC76 (c).

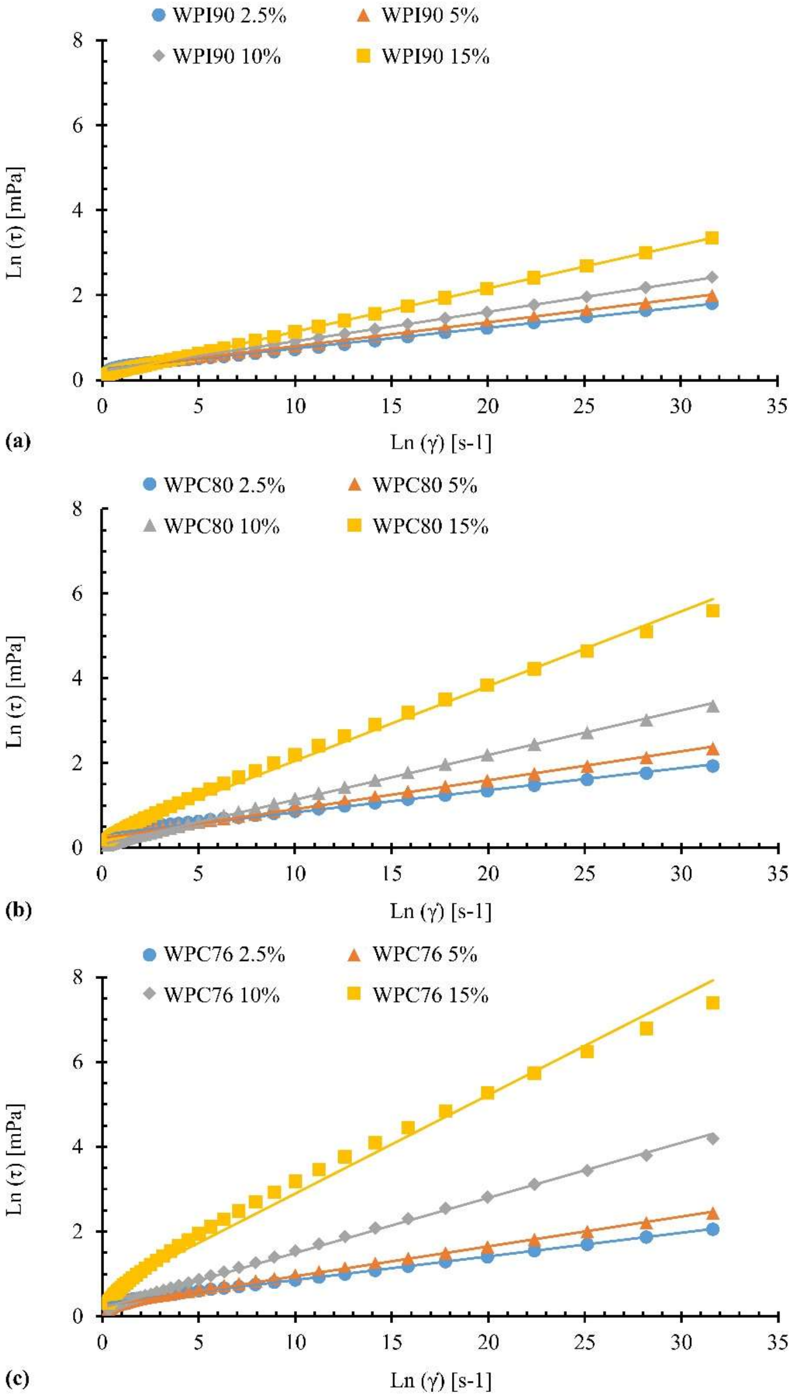


**Figure 5.** Flow curves of the RPO emulsions in Casson fluids model when stabilized by WPI90 (a), WPC80 (b), and WPC76 (c).

Previous studies have also reported shear-thinning behaviour for WP-stabilized emulsions (Drapala *et al*., 2017; Sun and Gunasekaran, 2009; Xi *et al*., 2019). Further, at high emulsifier concentrations, the produced emulsions clearly showed shear-thinning behaviour. Shearing force during analysis may have destroyed the droplet structure, or shearing may have aided oil flocculation, allowing shear-thinning behaviour to be observed (Derkach, 2009; Drapala *et al*., 2017).

The flow behaviours of the produced RPO emulsions were investigated, and the best suited models with the highest regression coefficient ($R^2$) values were chosen (numerical data not shown). Based on the results, except for the 15% WPC80- and WPC76-stabilized emulsions that followed the Herschel–Bulkley fluid model, almost all formed emulsions showed flow behaviours that suited the Casson fluid model. Contrariwise, Sun and Gunasekaran (2009) and Xi *et al*. (2019) found that the Power-law model adequately described the flow behaviour of 2% (w/w) WPI-stabilized emulsions. The Casson fluid model is commonly used to describe the behaviour of melted chocolate and chocolate milk, but it might also be used to cream/paste, liquid milk, and ice cream (Ačkar *et al*., 2015; Cropotova *et al*., 2017; Poursani *et al*., 2020). The Herschel–Bulkley model is a generalized model for describing the non-Newtonian behaviour of various fluid foods with shear-thinning properties (Tadros, 2013). The Herschel–Bulkley model explains the behaviour of shear-thinning fluids with a yield stress, which is a typical of complex fluids.

The emulsion made with 15% WPC80 and 15% WPC76 exhibited different physical properties than others; both had considerably varied flow behaviour characteristics. The flow curves of emulsions stabilized with 15% WPC80 and 15% WPC76 deviated in trend compared from the others (Figures 4a–c). The slope (steepness) of the Casson fluid flow differed significantly between emulsions stabilized by 15% WPC80 and 15% WPC76, as shown in Figures 4b and 4c. This slope indicates the Casson rheological constant ($\eta$), which is the specific force required to maintain a steady flow in the fluids, indicating the extent of shear-thinning behaviour of the emulsions formed. The results indicated that the 15% WPC80- and WPC76-stabilized emulsions required more force to maintain flow than the others.

Based on the Casson rheological constant ($\eta$) (Figure 1b and Figure 5) and the flow behaviour index ($n$) for Herschel–Bulkley fluid (Figure 1b), the influence of WP concentration on RPO emulsion flow behaviour could be detected. The $n$ in the Herschel–Bulkley fluid model, like the Casson rheological constant ($\eta$), specifies a shear-thinning “factor”. Nevertheless, despite the fact that a trend was discovered, the influence of WP type on RPO emulsion flow behaviour could not be significantly identified in this study (Figure 1b). In addition, the Casson rheological constant ($\eta$) and the Casson behaviour index (n) increased when the WP concentration was increased. According to the findings of this investigation, the intensity of shear-thinning behaviour increased with increasing WP concentration.

All RPO emulsions produced had yield stress (i.e., the Casson or Herschel–Bulkley yield stress). Further, the yield stress of the RPO emulsions produced varied without any discernible trend. The results showed that the WP type or concentration had no effect on the yield stress of the produced RPO emulsions.

***Physical stability of produced RPO emulsions***

Dynamic amplitude oscillatory shear measurement was done on the produced WP-based RPO emulsions in the shear range of 0.1%–1.000% to further evaluate the emulsion stability. Based on the amplitude range applied, the test performed in the range of short-amplitude oscillatory shear (0.1%–10%) to a large-amplitude oscillatory shear (10%–100%). Almost all RPO emulsions formed had $G''$ higher than $G'$ over the range of strain tested, and no curve intersection or flow point was found (Table 2). This study results indicated that the RPO emulsions formed were primarily viscous. However, the 15% WPI90-stabilized emulsion exhibited a crossover point between its $G''$ and $G'$ at 4% strain tested. After 4% strain was applied, this implied that the 15% WPI90-stabilized emulsion transformed to primarily elastic behaviour (which may result in emulsion-gel form) at higher strain applied.

At high strain applied, the emulsion's $G'$ curves collapsed (was observed to decrease). This set a limit for the linear viscoelastic range (*LVE*) of the emulsions. The *LVE* range limit is the regime in which the elastic modulus remains constant until a certain "critical strain" point is reached. The *LVE* values may be used to evaluate the emulsions' resistance to deformation. The lower the *LVE* number, the less stable the emulsion since it is easier to deform (e.g., experience droplet break up) with lower force exposure.

**Table 2.** Viscoelastic properties and stability of the RPO emulsions based on dynamic amplitude oscillatory shear tests.

| WP type | *c* (%) | Characteristic | |
|---|---|---|---|
| | | Viscoelastic Properties | *LVE* Limit (%)* |
| WPI90 | 2.5 | G">>G' | $0.22^a$ |
| | 5 | G">>G' | $0.31^a$ |
| | 10 | G">>G' | $0.32^a$ |
| | 15 | G">>G' | $0.49^a$ |
| WPC80 | 2.5 | G">>G' | $0.48^a$ |
| | 5 | G">>G' | $0.80^a$ |
| | 10 | G">>G' | $0.83^a$ |
| | 15 | G">>G' | $3.20^a$ |
| WPC76 | 2.5 | G">>G' | $0.23^a$ |
| | 5 | G">>G' | $0.32^a$ |
| | 10 | G">>G' | $1.30^a$ |
| | 15 | G">>G' | $7.90^a$ |

*Different superscript letters (a, b, and c) indicate significant difference ($p < 0.05$)

The *LVE* of the RPO emulsions in this study varied (Table 2). Except for the WPI90-stabilized emulsions, the *LVE* increased with the WP concentration used. Meanwhile, the 15% WPC76-stabilized emulsion exhibited the highest LVE and significantly differed from the others. The results implied that the 15% WPC76-

stabilized RPO emulsion showed the highest physical stability against applied strain. This work findings are consistent with prior research (Armetha *et al*., 2022), which found that 15% WPC76-stabilized emulsions had the best physical stability of any emulsion tested.

Nevertheless, the *LVE* in this study was close to the lowest strain in the range tested (≈0.1%). Because of this, it was unable to analyse the emulsion characteristics produced throughout the entire *LVE* range. The high proportion of the oil phase in the produced RPO emulsions might explain the tendency of short-limited LVE range in this study. Previous research has found that the size of the *LVE* region decreases with increasing oil phase volume fraction because emulsions may undergo a behaviour transition from predominantly entropic behaviour to predominantly enthalpy behaviour (Dickinson and Chen, 1999; Sun and Gunasekaran, 2009). However, *LVE* analysis is still useful in explaining the stability of WP stabilized RPO emulsions with high oil fraction, as revealed in this study. Further researcher into the *LVE* range limit for small amplitude oscillatory shear with a lower strain range (<0.1%) may be needed.

## Conclusions

Rheological characterisations were used to evaluate the physical stability of WP-stabilized RPO emulsions in this study. Other parameters of physical properties, such as $D_{10}$, $D_{50}$, and $D_{90}$, ζ potential, and electrical conductivity ($k$), became interrelated with rheological properties in explaining the observed physical emulsion stability. The results showed that the WP type and concentration had an influence on the rheological properties and other physical characteristics. Nevertheless, the emulsifier type and concentration were not the only determinants, given the complexity of an emulsion system. The shear-thinning flow behaviour and predominantly viscous characteristics of the WP-stabilized RPO emulsions were observed in this study. The flow behaviour of the produced RPO emulsions predominantly fitted the Casson fluid model, with the exception of the 15% WPC80- and WPC76-stabilized emulsions that fitted the Herschel–Bulkley fluid model. In addition, the 15% WPC76-stabilized RPO emulsion showed the best physical stability.

## Acknowledgments

This work was supported by Glanbia Nutritionals (for providing commercially available WPs) and PT Equiva Ligand Indonesia (for the access to the analytical equipment MCR 92 series), and was funded by a PMDSU research grant from The Indonesian Ministry of Higher Education and Culture.

## References

Ačkar, D., Škrabal, S., Šubarić, D., Babić, J., Miličević, B., Jozinović, A. 2015. Rheological properties of milk chocolates as influenced by milk powder type, emulsifier, and cocoa butter equivalent additions. *International Journal of Food Properties*, **18**(7), 1568–1574.

Adjonu, R., Doran, G., Torley, P., Agboola, S. 2014. Formation of whey protein isolate hydrolysate stabilised nanoemulsion. *Food Hydrocolloids*, **41**, 169–177.

Anton Paar. 2017. LitesizerTM Series Instruments.

Armetha, V., Hariyadi, P., Sitanggang, A.B., Yuliani, S. 2022. Physical characterization of red palm oil emulsion. *Proceedings of the 6th Food Ingredient Asia Conference - 6th FiAC*, ISBN 978-989-758-540-1, 185-190.

Barnes, H.A. 2000. A handbook of elementary rheology (Vol. 1). Aberystwyth: University of Wales, Institute of Non-Newtonian Fluid Mechanics.

Boon, C.S. 2009. Factors influencing the stability of carotenoids in oil-in-water emulsions. *Dissertation*. University of Massachusetts Amherst.

Burri, B.J. 2012. Evaluating global barriers to the use of red palm oil as an intervention food to prevent vitamin A deficiency. *Comprehensive Reviews in Food Science and Food Safety*, **11**(2), 221–232.

Castel, V., Rubiolo, A.C., Carrara, C.R. 2017. Droplet size distribution, rheological behavior and stability of corn oil emulsions stabilized by a novel hydrocolloid (Brea gum) compared with gum arabic. *Food Hydrocolloids*, **63**, 170–177.

Cropotova, J., Popel, S., Draganova, E., Parshakova, L., Colesnicenco, A. 2017. The use of seedless grape varieties for developing dairy-free creams. *The Annals of the University Dunarea de Jos of Galati. Fascicle VI-Food Technology*, **41**(2), 127–140.

Derkach, S.R. 2009. Rheology of emulsions. *Advances in Colloid and Interface Science*, **151**(1–2), 1–23.

Dickinson, E., Chen, J. 1999. Heat-set whey protein emulsion gels: Role of active and inactive filler particles. *Journal of Dispersion Science and Technology*, **20**(1–2), 197–213.

Domian, E., Brynda-Kopytowska, A., Oleksza, K. 2015. Rheological properties and physical stability of o/w emulsions stabilized by OSA starch with trehalose. *Food Hydrocolloids*, **44**, 49–58.

Drapala, K.P., Auty, M.A.E., Mulvihill, D.M., O'Mahony, J.A. 2017. Influence of emulsifier type on the spray-drying properties of model infant formula emulsions. *Food Hydrocolloids*, **69**, 56–66.

Drapala, K.P., Mulvihill, D.M., O'Mahony, J.A. 2018. A review of the analytical approaches used for studying the structure, interactions and stability of emulsions in nutritional beverage systems. *Food Structure*, **16**, 27–42.

Ha, H.K., Rankin, S.A., Lee, M.R., Lee, W.J. 2019. Development and characterization of whey protein-based nano-delivery systems: A review. *Molecules*, **24**(18), 1–17.

Hinderink, E.B.A., Schröder, A., Sagis, L., Schroën, K., Berton-Carabin, C.C. 2021. Physical and oxidative stability of food emulsions prepared with pea protein fractions. *LWT - Food Science and Technology*, **146**, 111424.

Loganathan, R., Subramaniam, K.M., Radhakrishnan, A.K., Choo, Y.M., Teng, K.T. 2017. Health-promoting effects of red palm oil: Evidence from animal and human studies. *Nutrition Reviews*, **75**(2), 98–113.

Mantovani, R.A., Cavallieri, Â.L.F., Netto, F.M., Cunha, R.L. 2013. Stability and in vitro digestibility of emulsions containing lecithin and whey proteins. *Food and Function*, **4**(9), 1322–1331.

McClements, D.J. 2004. Protein-stabilized emulsions. *Current Opinion in Colloid and Interface Science*, **9**(5), 305–313.

McClements, D.J. 2007. Critical review of techniques and methodologies for characterization of emulsion stability. *Critical Reviews in Food Science and Nutrition*, **47**(7), 611–649.

McClements, D.J., Decker, E.A., Weiss, J. 2007. Emulsion-based delivery systems for lipophilic bioactive components. *Journal of Food Science*, **72**(8), R109-124.

Mohamad, W.A.F.W., McNaughton, D., Buckow, R., Augustin, M.A. 2017. Stability and partitioning of β-carotene in whey protein emulsions during storage. *Food and Function*, **8**(11), 3917–3925.

Pelegrine, D.H.G., Gasparetto, C.A. 2005. Whey proteins solubility as function of temperature and pH. *LWT - Food Science and Technology*, **38**(1), 77–80.

Poursani, P., Razavi, S.M.A., Tehrani, M.M., Javidi, F. 2020. Rheological, physical, and sensory properties of non-fat ice creams as affected by selected fat replacers. *Journal of Food Processing and Preservation*, 1–11.

Ricaurte, L., Perea-Flores, M.D.J., Martinez, A., Quintanilla-Carvajal, M.X. 2016. Production of high-oleic palm oil nanoemulsions by high-shear homogenization (microfluidization). *Innovative Food Science and Emerging Technologies*, **35**, 75–85.

Sun, C., Gunasekaran, S. 2009. Effects of protein concentration and oil-phase volume fraction on the stability and rheology of menhaden oil-in-water emulsions stabilized by whey protein isolate with xanthan gum. *Food Hydrocolloids*, **23**(1), 165–174.

Tadros, T.F. 2013. *Emulsion Formation and Stability* (T. F. Tadros (ed.)). Wiley-VCH Verlag.

Xi, Z., Liu, W., McClements, D.J., Zou, L. 2019. Rheological, structural, and microstructural properties of ethanol induced cold-set whey protein emulsion gels: Effect of oil content. *Food Chemistry*, **291**, 22–29.

Yang, J., Thielen, I., Berton-Carabin, C.C., van der Linden, E., Sagis, L.M.C. 2020. Nonlinear interfacial rheology and atomic force microscopy of air-water interfaces stabilized by whey protein beads and their constituents. *Food Hydrocolloids*, **101**, 105466.

Zhu, Y., Gao, H., Liu, W., Zou, L., McClements, D.J. 2020. A review of the rheological properties of dilute and concentrated food emulsions. *Journal of Texture Studies*, **51**(1), 45–55.